

ICOS: Efficient and Highly Robust Point Cloud Registration with Correspondences

Lei Sun

Abstract—Point Cloud Registration is a fundamental problem in robotics and computer vision. Due to the limited accuracy in the matching process of 3D keypoints, the presence of outliers, probably in very large numbers, is common in many real-world applications. In this paper, we present ICOS (Inlier searching using COmpatible Structures), a novel, efficient and highly robust solution for the correspondence-based point cloud registration problem. Specifically, we (i) propose and construct a series of compatible structures for the registration problem where various invariants can be established, and (ii) design two time-efficient frameworks, one for known-scale registration and the other for unknown-scale registration, to filter out outliers and seek inliers from the invariant-constrained random sampling built upon the compatible structures. In this manner, even with extreme outlier ratios, inliers can be detected and collected for solving the optimal transformation, leading to our robust registration solver ICOS. Through plentiful experiments over standard real datasets, we demonstrate that: (i) our solver ICOS is fast, accurate, robust against as many as 99% outliers with nearly 100% recall ratio of inliers whether the scale is known or unknown, outperforming other state-of-the-art methods, (ii) ICOS is practical for use in real-world applications.

Index Terms—Point cloud registration, robust estimation, invariants, compatibility, graduated non-convexity

I. INTRODUCTION

POINT cloud registration is a cornerstone in robotics and computer vision, and has been broadly applied in scene reconstruction [7], [10], [19], object localization and recognition [14], [17], [29], medical imaging [3], Simultaneous Localization and Mapping (SLAM) [41], etc. It aims to estimate the transformation (scale, rotation and translation) between two 3D point clouds from the putative point correspondences.

Iterative Closest Point (ICP) [6] is a popular local-minimum registration approach but is too dependent on the initial guess of the transformation, thus prone to fail without a promising initialization. Therefore, an initialization-free way to address the registration problem—to build correspondences between point clouds from 3D keypoints [34], has grown increasingly popular. Many correspondence-based methods [2], [8], [9], [20], [38], [39], [43] have been proposed to solve the registration problem in the presence of noise.

However, there exists a difficulty for these correspondence-based approaches. In real-world scenes, the input correspondences are very likely to be corrupted by outliers, because, unlike the 2D keypoint matchers (e.g. SIFT [25] and SURF [5]) that can be relatively more stable and robust, the 3D keypoint detecting and matching methods (e.g. [31], [35]) may generate

Lei Sun is with the School of Mechanical and Power Engineering, East China University of Science and Technology, Shanghai 200237, P.R.China; e-mail: (leisunjames@126.com).

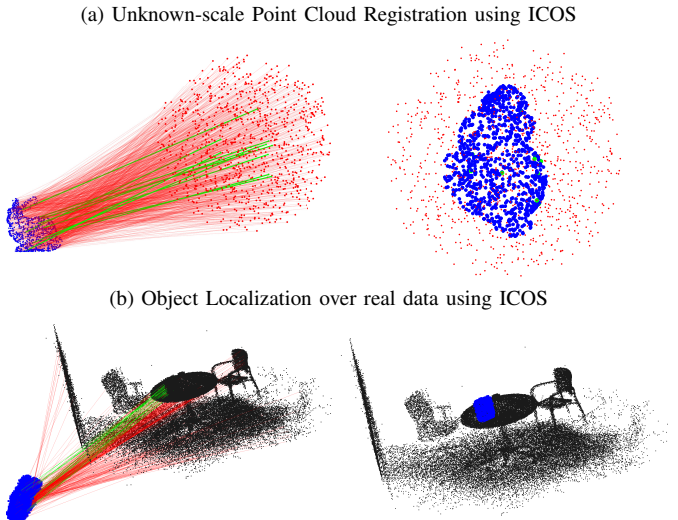


Fig. 1. 3D Point Cloud Registration Problems using ICOS. (a) Unknown-scale registration. Left: Among the 1000 putative correspondences, there exist 990 outliers (red lines) and merely 10 inliers (green lines). Right: Our solver ICOS can still estimate the scale, rotation and translation robustly and precisely. (b) Object localization with unknown scale in a realistic scene. Left: Correspondences are built between the object and the RGB-D scene [40] with 92% outliers. Right: ICOS can accurately reproject the object back to the scene with the transformation it estimated.

mismatched or spurious results due to noise, repetitive patterns, low-textured scenes, etc. Therefore, for real applications, robust registration methods are of paramount importance.

When it comes to robust estimation, RANSAC [16] is a common robust heuristic [1], but it has a critical disadvantage: its runtime increases exponentially with the outlier ratio among the correspondences, hence impractical for use when encountering the extreme outlier ratios (e.g. more than 90%). Besides, though the guaranteed outlier removal method GORE [9] as well as the non-minimal solutions FGR [43] and TEASER/TEASER++ [38], [39] have been proposed to deal with point cloud registration problems with over 90% outliers, they only succeed when the scale between the two point clouds is known and fixed. Nonetheless, when the scale varies (e.g. in cross-source point cloud registration problems), none of these methods could tolerate more than 90% outliers, which indeed necessitates a general solver capable of handling not only the known-scale problems but the unknown-scale ones.

Our Contributions. Motivated by this fact, in this paper we propose a novel robust solver, named ICOS (Inlier searching with COmpatible Structures) for solving both the known-scale and unknown-scale point cloud registration with extreme outlier ratios.

To be specific, ICOS aims to seek the correct inliers (rather than pruning outliers as in previous works [9], [32]) through

the random sample flow, but significantly different from the RANSAC-family (e.g. [12], [16], [23]), the sampling and filtering process of ICOS is built upon and also improved by the constraints derived from the *compatible structures* that we define based on the theory of *invariance*.

First, we introduce and construct a series of *compatible structures* for the point cloud registration problem, with which we are able to ‘customize’ special invariant-based constraints (or conditions) that can be used for effectively differentiating inliers from outliers only using simple Boolean conditions (Section IV).

In addition, we design two random-sampling-based frameworks that can fit with the compatible structures to seek and preserve eligible inliers from the putative correspondences for both known-scale and unknown-scale registration, in which different sampling strategies are employed to make our solver as time-efficient and practical as possible (Section V).

Finally, we validate the resulting solver ICOS in a variety of experiments over different datasets and show that: (i) ICOS is precise and robust even when 990 of 1000 correspondences are outliers in both known-scale and unknown-scale registration problems, (ii) ICOS runs fast, yields accurate estimates and recalls approximately 100% of the inliers, and (iii) it is also applicable to object localization in real 3D scenes (Section VI).

II. RELATED WORK

In this section, we provide some reviews on: (i) methods for building point correspondences, (ii) typical correspondence-based registration solvers by dividing them into two categories: the naive (outlier-free) ones and the robust ones, and (ii) typical robust heuristics for outlier rejection.

Building Point-to-point Correspondences. Generally, the point-to-point correspondences between two point clouds are first detected and then matched by the 3D feature descriptors, where some typical examples include FPFH [31], ISS [42] and FCGF [11]. But the drawback of these 3D descriptors are their comparatively low accuracy and robustness, which could result in very high or even extreme outlier ratios in some real-world scenes, as has been discussed in [9]. And this is exactly why the correspondence-based registration solvers should be made as insensitive to outliers as possible.

Naive Registration Solvers. Naive point cloud registration problems can be solved using closed-form solutions [2], [20] by decoupling the estimation of rotation, scale and translation. Besides, Branch-and-Bound (BnB) has also been applied to solve the registration problem [28] in a globally optimal way. And more recently, the Lagrangian Dual Relaxation is developed to produce a globally optimal generalized registration solver [8] for handling point-to-point, point-to-line and point-to-plane registration with good optimality guarantees. But the above-mentioned solutions will be unsuccessful once there are outliers among the correspondences.

Robust Registration Solvers. The minimal closed-form solutions can be fit into the RANSAC-family frameworks [12], [16], [23] to deal with outliers, though may be slow when the outlier ratio is high. Another idea to become robust is that: if outliers can be guaranteed to be removed or eliminated as many as possible, then what still remain should

be mostly inliers. GORE [9] is such a preprocessing outlier removal approach that guarantees that the correspondences removed must not be inliers. In terms of the non-minimal robust solvers, FGR [43] is the first method using Graduated Non-Convexity (GNC) to reject outliers, which estimates the rigid transformation matrix with a Gauss-Newton method. Though not globally optimal, FGR is efficient for known-scale registration. Currently, TEASER/TEASER++ [38], [39] are the more robust non-minimal certifiably globally optimal solvers that can dispose of 99% outliers in the known-scale situation. Another recent solution [24] utilizes RANSAC for scale and translation estimation, and also adopt the GNC framework to solve the rotation. Unfortunately, all these solvers are either incapable of estimating the scale or unable to tolerate over 90% outliers for unknown-scale point cloud registration (as will be shown in Fig. 5).

Robust Heuristics. RANSAC is a very classic hypothesize-and-test heuristic, which usually requires minimal solvers (or very fast non-minimal solvers) to obtain the best consensus set through random sampling. Its limitation lies in its exponentially increasing runtime w.r.t. the outlier ratio. Moreover, M-estimation is useful for outlier rejection [21], [26], [27], [43]. When the naive solver is non-minimal, the special M-estimator GNC [37] is a general-purpose heuristic operated by alternating optimization and adopts robust cost functions like Geman-McClure (GM) or Truncated Least Squares (TLS), which can typically handle 70-80% outliers in many robotic or computer vision problems. In addition, invariants or graph theory can be also applied for robust estimation. The methodologies mainly include: (i) to first prune outliers and then hand the rest of the correspondences over to other heuristics or solvers [32], [38], [39], and (ii) to first seek a portion of inliers, make an estimate, and then use the solutions to find the complete inlier set [33]. Our work has spirits closest to the latter.

III. PROBLEM FORMULATION

With two 3D point sets $\mathcal{P} = \{\mathbf{P}_i\}_{i=1}^N$ and $\mathcal{Q} = \{\mathbf{Q}_i\}_{i=1}^N$ in the correspondence-based point cloud registration problem, where we consider tuple $(\mathbf{P}_i, \mathbf{Q}_i)$ as a point correspondence, we can have the following relation:

$$s\mathbf{R}\mathbf{P}_i + \mathbf{t} + \boldsymbol{\varepsilon}_i = \mathbf{Q}_i, \quad (1)$$

where $s > 0$ is the scale, $\mathbf{R} \in SO(3)^1$ is the rotation matrix, $\mathbf{t} \in \mathbb{R}^3$ is the translation vector, and $\boldsymbol{\varepsilon}_i \in \mathbb{R}^3$ represents the measurement of Gaussian noise with isotropic covariance $\sigma^2\mathbf{I}_3$ (σ is the standard deviation and $\mathbf{I}_3 \in \mathbb{R}^{3 \times 3}$ is the identity matrix) and mean $\mu = 0$ w.r.t. the i_{th} correspondence. We then define a point cloud registration problem with scale below.

Problem 1 (Point Cloud Registration with Scale): Solving the point cloud registration problem with scale under the perturbation of noise is equivalent to the following minimization problem:

$$\min_{s>0, \mathbf{R} \in SO(3), \mathbf{t} \in \mathbb{R}^3} \sum_{i=1}^N \|s\mathbf{R}\mathbf{P}_i + \mathbf{t} - \mathbf{Q}_i\|^2, \quad (2)$$

¹The explicit expression about $SO(3)$ can be found in [8], [36].

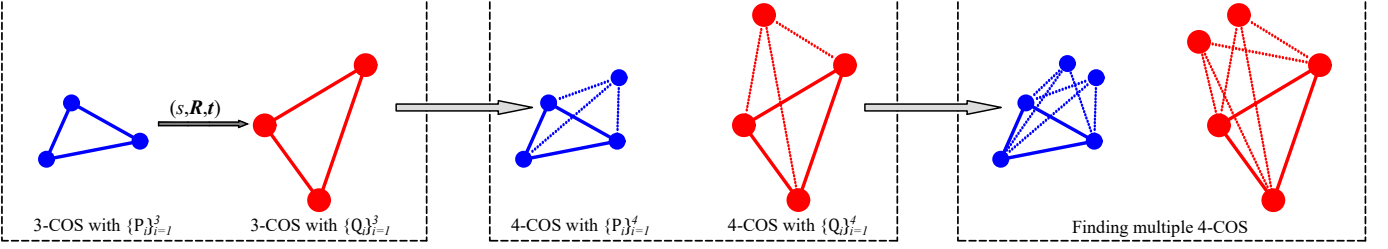


Fig. 2. Overview of the inlier searching process of ICOS. We start by finding eligible 3-COS across the two point sets, then seek new correspondences that can form 4-COS with the existing 3-COS, and eventually stop sampling when we collect a sufficient number of 4-COS.

where global minimizers $(\hat{s}, \hat{\mathbf{R}}, \hat{\mathbf{t}})$ are the optimal solutions to this registration problem.

When the scale aligning the two point clouds is fixed, which means $s = 1$, we can directly omit s in Problem 1, called the *known-scale* registration problem. However, the scale could vary, which, for instance, exists in the cross-source point cloud registration problem. In this case, the scale needs to be estimated additionally, and such problems are called *unknown-scale* registration, which is also the generalized version of point cloud registration. Our work intends to solve both the known-scale and the unknown-scale registration in the presence of both noise and a great number of outliers among the putative correspondences, providing a highly robust backend for real applications.

IV. COMPATIBLE STRUCTURES IN THE POINT CLOUD REGISTRATION PROBLEM

We first define the *compatible structures* (abbreviated as ‘COS’ in the rest of the paper) for the point cloud registration problem, and then explore the potential invariants among them.

Definition 1 (3-COS and Pairwise Scale-based Invariants): Assume that we have 3 non-collinear point correspondences $(\mathbf{P}_i, \mathbf{Q}_i), i = 1, 2, 3$, defined as one 3-COS. We can derive the following pairwise scale(length)-based invariants²:

$$I_{ij}^s = \frac{\|\mathbf{Q}_i - \mathbf{Q}_j\|}{\|\mathbf{P}_i - \mathbf{P}_j\|} = s_{gt} + \epsilon_{ij}, \quad (3)$$

where $(i, j) \in \{(1, 2), (1, 3), (2, 3)\}$, I_{ij}^s represents the scale-based invariant w.r.t. the i_{th} and the j_{th} correspondences, and s_{gt} denotes the ground-truth scale, and ϵ_{ij} denotes the noise measurement (disturbance) on this invariant.

Now we can further endow any pair of scale-based invariants I_{ij}^s with the constraint given as follows.

Proposition 1 (Constraints on I_{ij}^s): For any two invariants I_{ij}^s in the 3-COS above, we can derive that

$$|I_{ij}^s - I_{jk}^s| \leq A \left(\frac{1}{\|\mathbf{P}_i - \mathbf{P}_j\|} + \frac{1}{\|\mathbf{P}_j - \mathbf{P}_k\|} \right) \quad (4)$$

where $(i, j, k) \in \{(1, 2, 3), (2, 3, 1), (3, 1, 2)\}$ (here I_{ij}^s and I_{ji}^s denote the same invariant), and A is the noise bound, satisfying that $2\|\epsilon\| \leq A$. In addition, when the scale is known ($s_{gt} = 1$), we can further have that

$$|I_{ij}^s - 1| \leq A \left(\frac{1}{\|\mathbf{Q}_i - \mathbf{Q}_j\|} \right). \quad (5)$$

²The explicit definition of invariants in geometric vision problems can be seen in [32], [33].

Proof 1: It is easy to have that

$$s_{gt} \mathbf{R}_{gt} \mathbf{P}_{ij} + \epsilon_{ij} = \mathbf{Q}_{ij}, \Rightarrow \|s_{gt} \mathbf{R}_{gt} \mathbf{P}_{ij}\| = \|\mathbf{Q}_{ij} - \epsilon_{ij}\|, \quad (6)$$

where $\mathbf{P}_{ij} = \mathbf{P}_i - \mathbf{P}_j$, $\mathbf{Q}_{ij} = \mathbf{Q}_i - \mathbf{Q}_j$, and $\epsilon_{ij} = \epsilon_i - \epsilon_j$. And using the triangular inequality, we can derive that

$$\|\mathbf{Q}_{ij}\| - \|\epsilon_{ij}\| \leq \|s_{gt} \mathbf{R}_{gt} \mathbf{P}_{ij}\| = s_{gt} \|\mathbf{P}_{ij}\| \leq \|\mathbf{Q}_{ij}\| + \|\epsilon_{ij}\|, \quad (7)$$

so that

$$s_{gt} - \frac{\|\epsilon_{ij}\|}{\|\mathbf{P}_{ij}\|} \leq \frac{\|\mathbf{Q}_{ij}\|}{\|\mathbf{P}_{ij}\|} \leq s_{gt} + \frac{\|\epsilon_{ij}\|}{\|\mathbf{P}_{ij}\|}. \quad (8)$$

Thus, inequalities (4) and (5) can be derived as long as we have: $\|\epsilon_{ij}\| \leq \|\epsilon_i\| + \|\epsilon_j\| \leq A$ ($2\|\epsilon\| \leq A$).

Subsequently, we can roughly calculate the raw scale s_{raw} and rotation \mathbf{R}_{raw} that aligns the 3-COS w.r.t. the two point sets, where we can use the weighted-representation in [39] to compute the scale:

$$\hat{s} = \frac{1}{\sum_{k=1}^K \omega_k} \cdot \sum_{k=1}^K \omega_k I_k^s, \quad (9)$$

where $\omega_i = \frac{\|\tilde{\mathbf{P}}_{ij}\|^2}{A^2}$, and each I_k^s corresponds to one I_{ij}^s . Then, we use the fast SVD solver [2] to estimate the rotation by the following steps: (i) we first compute the centroids for the two point sets such that

$$\bar{\mathbf{P}} = \frac{\sum_{i=1}^M \mathbf{P}_i}{M}, \bar{\mathbf{Q}} = \frac{\sum_{i=1}^M \mathbf{Q}_i}{M}, \quad (10)$$

and (ii) then we use SVD (Singular Value Decomposition) to solve the rotation and estimate the translation such that

$$\begin{aligned} \mathbf{U} \Sigma \mathbf{V}^\top &= SVD \left(\sum_{i=1}^M (\mathbf{P}_i - \bar{\mathbf{P}})(\mathbf{Q}_i - \bar{\mathbf{Q}})^\top \right), \\ \hat{\mathbf{R}} &= \mathbf{V} \mathbf{U}^\top, \\ \hat{\mathbf{t}} &= \bar{\mathbf{Q}} - \hat{s} \hat{\mathbf{R}} \bar{\mathbf{P}}. \end{aligned} \quad (11)$$

For the 3-COS problems, we adopt $M = 3$ and $K = 3$ and use \mathbf{R}_{raw} and \mathbf{t}_{raw} to represent rotation and translation instead.

Afterwards, we can define a new set of invariants based on the translation.

Definition 2 (Translation-based Invariants): In addition to (3), we can further derive the following translation-based invariants:

$$I_i^t = \mathbf{Q}_i - s_{raw} \mathbf{R}_{raw} \mathbf{P}_i = \mathbf{t}_{gt} + \zeta_i, \quad (12)$$

where $i \in \{1, 2, 3\}$, I_i^t represents the translation-based invariant w.r.t. the i_{th} correspondences, and ζ_i describes the noise measurement disturbance. In the known-scale cases, $s_{raw} = 1$.

Proposition 2 (Constraints on I_i^t): For invariants I_i^t in the 3-COS above, we can derive that

$$\|I_i^t - I_j^t\| \leq B \quad (13)$$

where $(i, j) \in \{(1, 2), (2, 3), (3, 1)\}$, and B is the noise bound, meaning that $2\|\zeta\| \leq B$.

Proof 2: The proof here is trivial.

Up to now, we have explored all the possible invariants as well as their constraints based on the rigid compatibility of the 3-COS. On the basis of this 3-COS, whenever we obtain a new correspondence as the fourth node, defined as a 4-COS, additional constraints can be further imposed as follows.

Proposition 3 (4-COS, Invariants and Constraints): If we have a new correspondence, say the 4_{th} one, in addition to the 3-COS we have, as shown in Fig. 2, we can build 3 more scale-based invariants such that

$$I_{i4}^s = \frac{\|\mathbf{Q}_i - \mathbf{Q}_4\|}{\|\mathbf{P}_i - \mathbf{P}_4\|} = s_{gt} + \epsilon_{i4}, \quad (14)$$

where $i \in \{1, 2, 3\}$, with the following constraints:

$$|I_{i4}^s - I_{j4}^s| \leq A \left(\frac{1}{\|\mathbf{P}_i - \mathbf{P}_4\|} + \frac{1}{\|\mathbf{P}_j - \mathbf{P}_4\|} \right), \quad (15)$$

where $i, j \in \{1, 2, 3\}, i \neq j$. Apart from simply constraining the scale-based rigidity, we also supplement a residual-based constraint on $(\mathbf{P}_4, \mathbf{Q}_4)$ such that

$$\|\bar{I}_{123}^s \mathbf{R}_{123} \mathbf{P}_4 + \bar{I}_{123}^t - \mathbf{Q}_4\| \leq C, \quad (16)$$

where \bar{I}_{123}^s and \bar{I}_{123}^t denote the mean scale and translation computed from the 3-COS as

$$\bar{I}_{123}^s = \frac{I_{12}^s + I_{13}^s + I_{23}^s}{3}, \quad \bar{I}_{123}^t = \frac{I_1^t + I_2^t + I_3^t}{3} \quad (17)$$

and C is the bound for this residual error. For the known-scale cases, $\bar{I}_{123}^s = 1$ is adopted. Moreover, for every single 3-COS in this 4-COS, we can compute a raw rotation, represented as \mathbf{R}_{ijk} for the correspondence tuple (i, j, k) . In this fashion, we are able to impose new constraints on the mutual compatibility between the raw rotations w.r.t. different correspondence tuples such that

$$\angle(\mathbf{R}_{ijk}, \mathbf{R}_{abc}) \leq D, \quad (18)$$

where ‘ \angle ’ is the geodesic error [18] between two rotations, given by

$$\angle(\mathbf{R}_{ijk}, \mathbf{R}_{abc}) = \left| \arccos \left(\frac{\text{tr}(\mathbf{R}_{ijk}^\top \mathbf{R}_{abc}) - 1}{2} \right) \right|, \quad (19)$$

$(i, j, k), (a, b, c) \in \{(1, 2, 3), (1, 2, 4), (1, 3, 4), (2, 3, 4)\}$, and $2\angle(\text{Exp}(\rho), \mathbf{I}_3) \leq D$ where ‘ Exp ’ is the exponential map [4] to define the effect of noise on the rotation, \mathbf{I}_3 means the 3×3 identity matrix, and D is the bound for the geodesic error.

Proof 3: The proof of constraints (15-16) is fairly apparent based on the derivations rendered above, thus omitted here.

Algorithm 1: ICOS for Known-scale Registration

Input : correspondences $\mathcal{P} = \{(\mathbf{P}_i, \mathbf{Q}_i)\}_{i=1}^N$;
minimum number of the inlier set size X ;
Output: optimal $(\hat{\mathbf{R}}, \hat{\mathbf{t}})$; inlier set \mathcal{P}^{In} ;

```

1 while true do
2    $\mathcal{P}^{In} \leftarrow \emptyset$ , count  $\leftarrow 0$ ;
3   for  $itr_1 = 1 : maxItr_1$  do
4     Randomly select  $\mathcal{R} = \{(\mathbf{P}_i, \mathbf{Q}_i)\}_{i=1}^2 \subset \mathcal{P}$ ;
5     if  $\mathcal{R}$  satisfies constraints (5) then
6       for  $itr_2 = 1 : maxItr_2$  do
7         Randomly select  $(\mathbf{P}_3, \mathbf{Q}_3) \in \mathcal{P}$  and
          construct a 3-COS set  $\mathcal{O}$ , with  $\mathcal{R}$ ;
8         if  $\mathcal{O}$  satisfies constraints (5) then
9           break
10        end
11      end
12      break
13    end
14  end
15  if  $\mathcal{O}$  satisfies constraints (4-5) then
16    Solve  $\mathbf{R}_{raw}$  with  $\mathcal{O}$  using (11);
17  if  $\mathcal{O}$  satisfies constraints (13) then
18    for  $itr_3 = 1 : maxItr_3$  do
19      checkSampling;
20      Randomly select  $(\mathbf{P}_k, \mathbf{Q}_k) \in \mathcal{P}$  and
        construct a 4-COS with  $\mathcal{O}$ ;
21      if this 4-COS satisfies (15-18) then
22        count = count + 1;
23         $\mathcal{P}^{In} \leftarrow \mathcal{P}^{In} \cup \{(\mathbf{P}_k, \mathbf{Q}_k)\}$ ;
24      end
25      if count  $\geq X$  then
26         $\mathcal{P}^{In} \leftarrow \mathcal{P}^{In} \cup \mathcal{O}$ ;
27        break
28      end
29    end
30  end
31 end
32 end
33 Solve  $(\hat{\mathbf{R}}, \hat{\mathbf{t}})$  with set  $\mathcal{P}^{In}$  using (11);
34 Compute residuals  $r_i$  ( $i = 1, 2, \dots, N$ ) for all the
correspondences in  $\mathcal{P}$ ; if  $r_i \leq 5.2\sigma$ , add it to  $\mathcal{P}^{In}$ ;
35 Solve optimal  $(\hat{\mathbf{R}}, \hat{\mathbf{t}})$  with  $\mathcal{P}^{In}$  using (11);
36 return optimal  $(\hat{\mathbf{R}}, \hat{\mathbf{t}})$  and the inlier set  $\mathcal{P}^{In}$ ;
```

For constraints (18), on the basis of the triangular inequality of the geodesic distance in [18], similar to [32], we can derive:

$$\begin{aligned}
\angle(\mathbf{R}_{ijk}, \mathbf{R}_{abc}) &= \angle(\text{RExp}(\rho_{ijk}), \text{RExp}(\rho_{abc})) \\
&= \left| \arccos \left(\frac{\text{tr}((\text{Exp}(\rho_{ijk})^\top \mathbf{R}^\top \text{RExp}(\rho_{abc}))) - 1}{2} \right) \right| \\
&= \angle(\text{Exp}(\rho_{ijk}), \text{Exp}(\rho_{abc})) \\
&\leq \angle(\text{Exp}(\rho_{ijk}), \mathbf{I}_3) + \angle(\text{Exp}(\rho_{abc}), \mathbf{I}_3) \leq D.
\end{aligned} \quad (20)$$

So far, we have derived the invariant-based constraints from 3-COS and 4-COS, leading to our robust registration solver.

Algorithm 2: ICOS for Unknown-scale Registration

Input : correspondences $\mathcal{P} = \{(\mathbf{P}_i, \mathbf{Q}_i)\}_{i=1}^N$;
 minimum number of the inlier set size X ;

Output: optimal $(\hat{s}, \hat{\mathbf{R}}, \hat{\mathbf{t}})$; inlier set \mathcal{P}^{In} ;

```

1 while true do
2    $\mathcal{P}^{In} \leftarrow \emptyset$ , count  $\leftarrow 0$ ;
3   Randomly select  $\mathcal{R} = \{(\mathbf{P}_i, \mathbf{Q}_i)\}_{i=1}^3 \subset \mathcal{P}$  as the
4     3-COS set  $\mathcal{O}$ ;
5   if  $\mathcal{O}$  satisfies constraints (4) then
6     Compute  $s_{raw}, \mathbf{R}_{raw}$  with  $\mathcal{O}$  using (9) (11);
7     if  $\mathcal{O}$  satisfies constraints (13) then
8       for  $itr_3 = 1 : maxItr_3$  do
9         checkSampling;
10        Randomly select  $(\mathbf{P}_k, \mathbf{Q}_k) \in \mathcal{P}$  and
11          construct a 4-COS with  $\mathcal{O}$ ;
12        if this 4-COS satisfies (15-18) then
13          count = count + 1;
14           $\mathcal{P}^{In} \leftarrow \mathcal{P}^{In} \cup \{(\mathbf{P}_k, \mathbf{Q}_k)\}$ ;
15        end
16        if count  $\geq X$  then
17           $\mathcal{P}^{In} \leftarrow \mathcal{P}^{In} \cup \mathcal{O}$ ;
18          break
19        end
20      end
21    end
22  end
23  Solve  $(\hat{s}, \hat{\mathbf{R}}, \hat{\mathbf{t}})$  with set  $\mathcal{P}^{In}$  using (9) and (11);
24  Compute residuals  $r_i$  ( $i = 1, 2, \dots, N$ ) for all the
25    correspondences in  $\mathcal{P}$ ; if  $r_i \leq 5.2\sigma$ , add it to  $\mathcal{P}^{In}$ ;
26  Solve optimal  $(\hat{s}, \hat{\mathbf{R}}, \hat{\mathbf{t}})$  with  $\mathcal{P}^{In}$  using (9) and (11);
27  return optimal  $(\hat{s}, \hat{\mathbf{R}}, \hat{\mathbf{t}})$  and the inlier set  $\mathcal{P}^{In}$ ;
```

V. OUR SOLVER: ICOS

In this section, we provide the complete overview of our solver ICOS for both the known-scale and the unknown-scale point cloud registration problems.

We first discuss the insights and the main structure of the proposed solver ICOS. As intuitively illustrated in Fig. 2, we begin with finding eligible 3-COS across the two point sets by roughly checking the scale-based invariants (4-5). Once a 3-COS satisfies the constraints on the scale, we solve the rotation and then the translation with it (although their accuracy has been greatly affected by noise). This is for further examining if the constraints on the translation-based invariants (13) are satisfied. Holding one eligible 3-COS, we then pick additional correspondences one after another with testing their residual-based constraints (16) and subsequently the rotation-based constraints (18), in order to further establish a 4-COS based on the 3-COS. The process of finding 4-COS continues until we are able to obtain a sufficient number of such 4-COS within reasonable times of the single-correspondence random sampling, which is another hidden condition serving to determine whether the 3-COS and its 4-COS could all be truly inliers.

The following subsections provide more details on formulating the pseudocode of ICOS.

Algorithm 3: *checkSampling* (Subroutine of ICOS)

Input : iteration number itr_3 , and $count$;

Output: **break** or **do nothing**;

```

1 if  $itr_3 \geq maxItr_4$  and  $count < 1$  then
2   | break
3 end
4 if  $itr_3 \geq 2maxItr_4$  and  $count < 2$  then
5   | break
6 end
7 if  $itr_3 \geq 3maxItr_4$  and  $count < 3$  then
8   | break
9 end
```

A. ICOS for Known-scale Registration

The pseudocode of ICOS for point cloud registration with known scale ($s = 1$) is given in Algorithm 1. We describe the detailed implementation procedures of ICOS as follows.

Lines 1-14: ICOS initiates with random sampling. But different from ordinary random sampling process, here we design a *decoupled sampling method*. First, we select random samples \mathcal{R} of 2 correspondences, rather than 3, and check if their scale-based invariant I_{12}^s is close enough to 1 using constraint (5). If it is, we can then proceed to select random samples for the remaining one correspondence, with which we try to form an eligible 3-COS that can satisfy constraints (5) based on \mathcal{R} ; if not, we continue our sampling to seek \mathcal{R} .

Lines 13-32: Once a qualified 3-COS (set \mathcal{O}) is obtained, we also check their constraints (4). If satisfied, we then solve the raw rotation with \mathcal{O} , and determine whether constraints (13) are fulfilled in \mathcal{O} . If yes, we then move on to sampling once again, in order to build one 4-COS based on the existing \mathcal{O} . We seek correspondences (one at a time) from random samples and feed them to \mathcal{O} sequentially to check constraints (15-18). When we collect enough correspondences (say X) that can construct qualified 4-COS with \mathcal{O} , we then stop sampling and return the $X+3$ inliers. During this sampling process, we add a subroutine *checkSampling*, which is designed to break from sampling when the obtained 3-COS \mathcal{O} does not seem to be inliers, and this could be realized by regularly checking the number of 4-COS formed according to the iteration number, as demonstrated in Algorithm 3.

Lines 33-35: Compute the solutions with the $X+3$ inliers and consider all correspondences whose residual errors satisfy $r_i \leq 5.2\sigma$ as inliers (σ denotes the standard deviation of the Gaussian noise). Finally, we can solve the optimal solutions with all the inliers found among the putative correspondences using the scale solver (9) as well as the fast non-minimal SVD transformation solver (11).

B. ICOS for Unknown-scale Registration

When the scale is unknown, ICOS would become different, and its pseudocode is shown in Algorithm 2.

Algorithm 2 utilizes the methodology similar to *lines 15-34* of Algorithm 1. The differences lie in that: (i) we are unable to impose constraints (5) on the 3-COS using the decoupled sampling method as operated in *lines 3-14*, since the scale is not fixed, which generally may require more runtime than the

known-scale problems, and (ii) the raw scale and the scale-based invariants cannot be set to 1, but need to be computed as in (3) and (14) instead.

C. Discussion on the Maximum Iteration Numbers

Note that in Algorithm (1-3), a series of maximum iteration numbers are involved w.r.t. the sampling process, so now we discuss their proper choice of values.

Generally, the maximum iteration we set can be given by the following formulation:

$$\max\text{It}\geq x \cdot \frac{\log(1-p)}{\log(1-(1-\text{outlier ratio})^n)}, \quad (21)$$

where x is the number of eligible inlier subsets desired, p is the confidence for the fact that all the correspondences selected are inliers (typically we choose $p = 0.98\text{-}0.99$), usually the outlier ratio should be within 0-99% (thus, 99% is typically chosen unless we can know in advance that the outlier ratio is below a certain level), and n is the number of correspondences we select for each random sample.

Therefore, for $\max\text{It}_1$, we adopt $n = 2$, choosing two correspondences at one time, while for $\max\text{It}_2$, $\max\text{It}_3$ and $\max\text{It}_4$, we all use $n = 1$ since they are for single-correspondence sampling.

D. Discussion on the Performance of ICOS

Since the main body of ICOS consists in simply judging a sequence of Boolean conditions (*true* or *false*) according to the constraints on invariants w.r.t. different variables, it can be fast to implement. Besides, ICOS abandon the strategy of making an estimate for every random sample selected (as in RANSAC), and solve the transformation smartly only when the scale-based constraints (4-5) allow it to. Also, residual errors w.r.t. all the correspondences are only required to solve once (for finding the whole inlier set), saving much time for practical implementation, particularly when the point cloud correspondences are in huge numbers, which is actually not uncommon in practice.

TABLE I

PARAMETER SETUP OF ICOS

Known-scale ICOS	Unknown-scale ICOS
$X = 4$	$X = 4$
$A = 4.5\sigma$	$A = 4.5\sigma$
$B = 5.0\sigma$	$B = 5.0\sigma$
$C = 6.0\sigma$	$C = 6.0\sigma$
$D = 10.5\sigma$	$D = 10.5\sigma$
$\max\text{It}_1 = 40000$	\
$\max\text{It}_2 = 400$	\
$\max\text{It}_3 = 1600$	$\max\text{It}_3 = 1600$
$\max\text{It}_4 = 400$	$\max\text{It}_4 = 400$

VI. EXPERIMENTS

In this section, we conduct a series of experiments based on multiple datasets to evaluate the proposed solver ICOS for point cloud registration, also in comparison with the existing state-of-the-art solvers. All the experiments are implemented in Matlab on a laptop with an i7-7700HQ CPU and 16GB RAM, and no parallelism programming is ever used.

A. Overall Benchmarking on Real Datasets

Experimental Setup. We evaluate our solver ICOS against other state-of-the-art methods over the ‘bunny’ and the ‘Armadillo’ point clouds from the Stanford 3D Scanning Repository [13]. We first randomly downsample the point cloud to 1000 points and resize it to be placed in a cube of $[-0.5, 0.5]^3$ meters, which can be regarded as the initial point set $\mathcal{P} = \{\mathbf{P}_i\}_{i=1}^{1000}$. Then, we generate a random rigid transformation: $(s, \mathbf{R}, \mathbf{t})$, in which scale $s \in [1, 5]$ meters, rotation $\mathbf{R} \in SO(3)$ and translation $\|\mathbf{t}\| \leq 3$ meters, to transform point set \mathcal{P} . We add random Gaussian noise with $\sigma = 0.01$ and $\mu = 0$ to the transformed point set, as the point set $\mathcal{Q} = \{\mathbf{Q}_i\}_{i=1}^{1000}$. To create outliers in clutter, a portion of the points in \mathcal{Q} are substituted by random points inside a sphere of diameter $s\sqrt{3}$ meters according to the outlier ratio (from 0% up to 99%), as exemplified in Fig. 3. All the experimental results are obtained over 50 Monte Carlo runs in the same environment.

The estimation errors in all experiments are computed as:

$$\begin{aligned} E_s &= |\hat{s} - s_{gt}|, \\ E_{\mathbf{R}} &= \angle(\hat{\mathbf{R}}, \mathbf{R}_{gt}), \\ E_{\mathbf{t}} &= \|\hat{\mathbf{R}} - \mathbf{R}_{gt}\|, \end{aligned} \quad (22)$$

where ‘ \angle ’ is the geodesic error (20) [18].

Known-scale problems: We adopt FGR, GORE, RANSAC, TEASER and ICOS for the known-scale point cloud registration problems. As for RANSAC, we use Horn’s minimal (3-point) method [20] to solve the rigid transformation and the confidence is set to 0.995. There are two stop conditions for RANSAC: (i) RANSAC with at most 1000 iterations, named RANSAC(1000), and (ii) RANSAC with at most 1 minute of runtime, named RANSAC(1min). In terms of TEASER, we adopt the GNC heuristic version as in [39] (using GNC to solve the large robust SDP problem), but differently: (i) we do not use parallelism programming in order to ensure the fairness of runtime for all the tested solvers, and (ii) it is completely implemented in Matlab, not C++, using the maximum clique solver [15]. The parameter setup for ICOS is given in Table I.

Unknown-scale problems: For unknown-scale registration, we only compare ICOS with RANSAC because: (i) FGR and GORE are not designed for scale estimation, and (ii) the scale estimator Adaptive Voting in TEASER is too slow for handling 1000 correspondences (tens of minutes per run) and is also unable to tolerate over 90% outliers (as will be shown in Fig. 5), thus no need for being compared.

Results. The main benchmarking results are shown in Fig. 3 (over the ‘bunny’) and Fig. 6 (over the ‘Armadillo’). We can observe that: (i) in the known-scale registration problem, though GORE, TEASER and our ICOS are all robust against 99% outliers, TEASER and ICOS are generally more accurate, (ii) RANSAC(1000) fails at 90%, while FGR and RANSAC(1min) fail at over 95%, and (iii) in the unknown-scale registration problems, ICOS can still address 99% outliers highly robustly, (iv) ICOS is the fastest solver when the outlier ratio is below 98% (Note that though FGR seems faster at over 96%, it has become no longer robust).

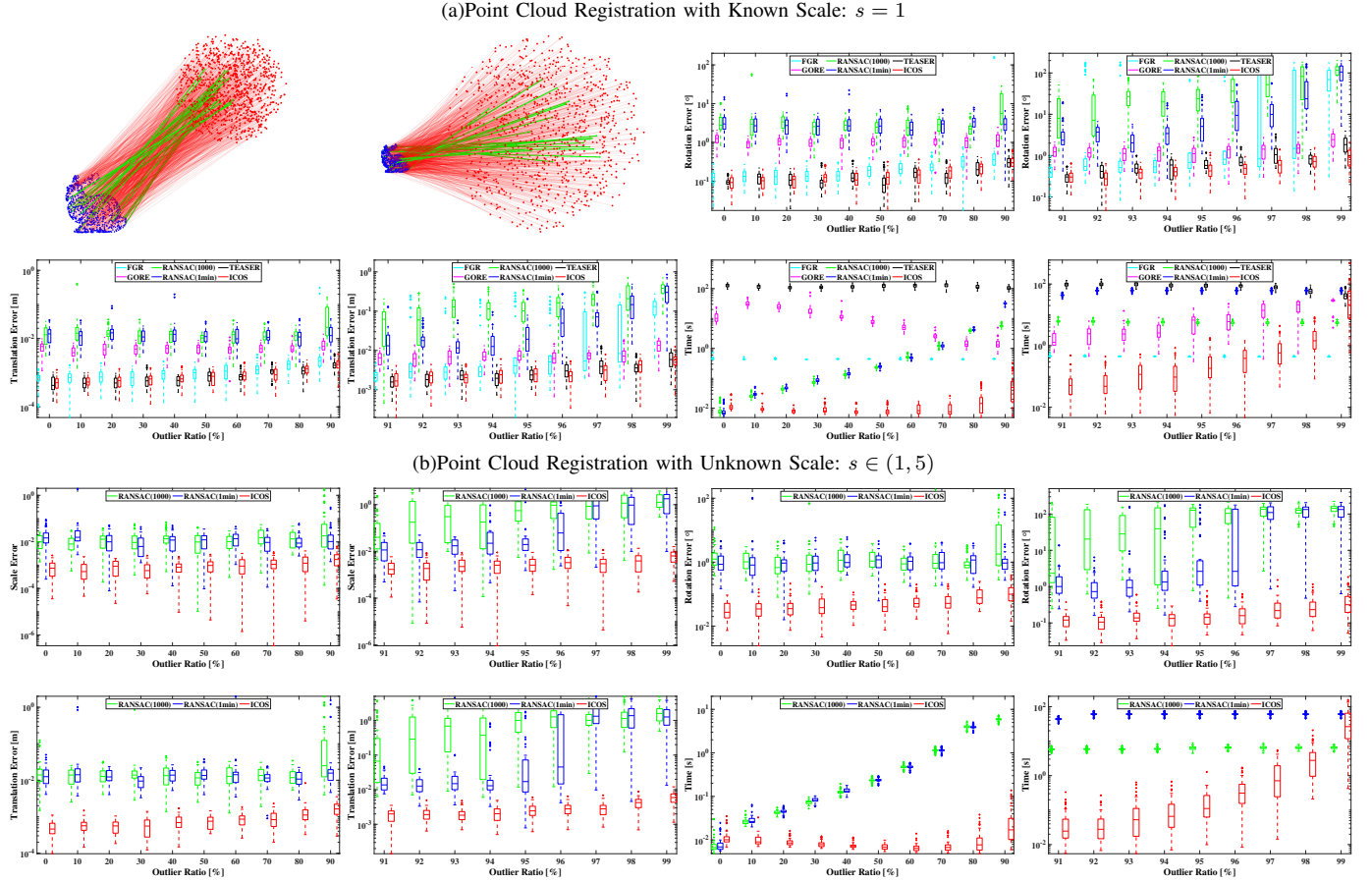


Fig. 3. Benchmarking on the ‘bunny’ [13]. Left-top: Examples of a known-scale and an unknown-scale point cloud registration problem with 98% outliers. (a) Known-scale registration results w.r.t. increasing outlier ratio (0-99%). (b) Unknown-scale registration results w.r.t. increasing outlier ratio (0-99%).

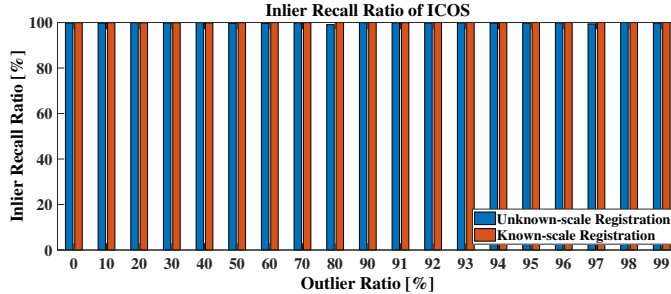


Fig. 4. Inlier recall ratio of ICOS in both the known-scale and the unknown-scale point cloud registration problems.

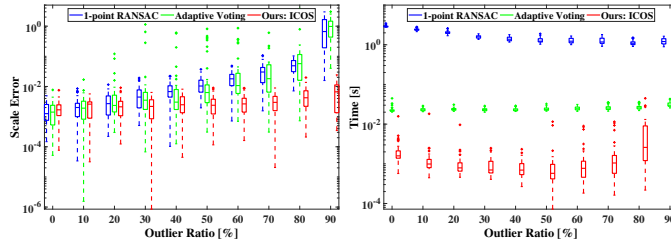


Fig. 5. Benchmarking on scale estimation. Left: Scale errors w.r.t. increasing outlier ratio (0-99%). Right: Runtime w.r.t. increasing outlier ratio (0-99%).

B. Evaluation on the Inlier Recall Ratio

We test the capability of ICOS to recall correct inliers from the outlier-corrupted putative correspondence set with the same experimental setup as in Section VI-A (with ‘bunny’),

and the results are shown in Fig. 4. The recall ratio is defined as the ratio of the number of true inliers found by ICOS in the end to the ground-truth number of inliers among all the correspondences. We can observe that ICOS is able to recall approximately 100% (no less than 99%) of the inliers from the correspondences with outlier ratio ranging from 0% to 99%, which underlies its high estimation accuracy against noise.

C. Benchmarking on Scale Estimation

We benchmark ICOS for scale estimation alone, compared with the Adaptive Voting in TEASER/TEASER++ and the 1-point RANSAC in [24]. Following the setup in Section VI-A, we further downsample the ‘bunny’ to 100 points because solver Adaptive Voting will run in tens of minutes with 1000 correspondences. In each run, the scale is randomly generated within (1, 5) meters. Fig. 5 shows the scale errors and the runtime w.r.t. increasing outlier ratio. We can see that both Adaptive Voting and 1-point RANSAC break at 90% outliers, while ICOS can stably tolerate 90% outliers and is faster than the other two competitors. In fact, ICOS is robust against 99% outliers, as has been shown in Section VI-A.

D. Qualitative Results over Real Datasets

In addition to the quantitative results rendered above, we provide qualitative results of registration problems over multiple real point clouds, including the ‘bunny’ and ‘Armadillo’

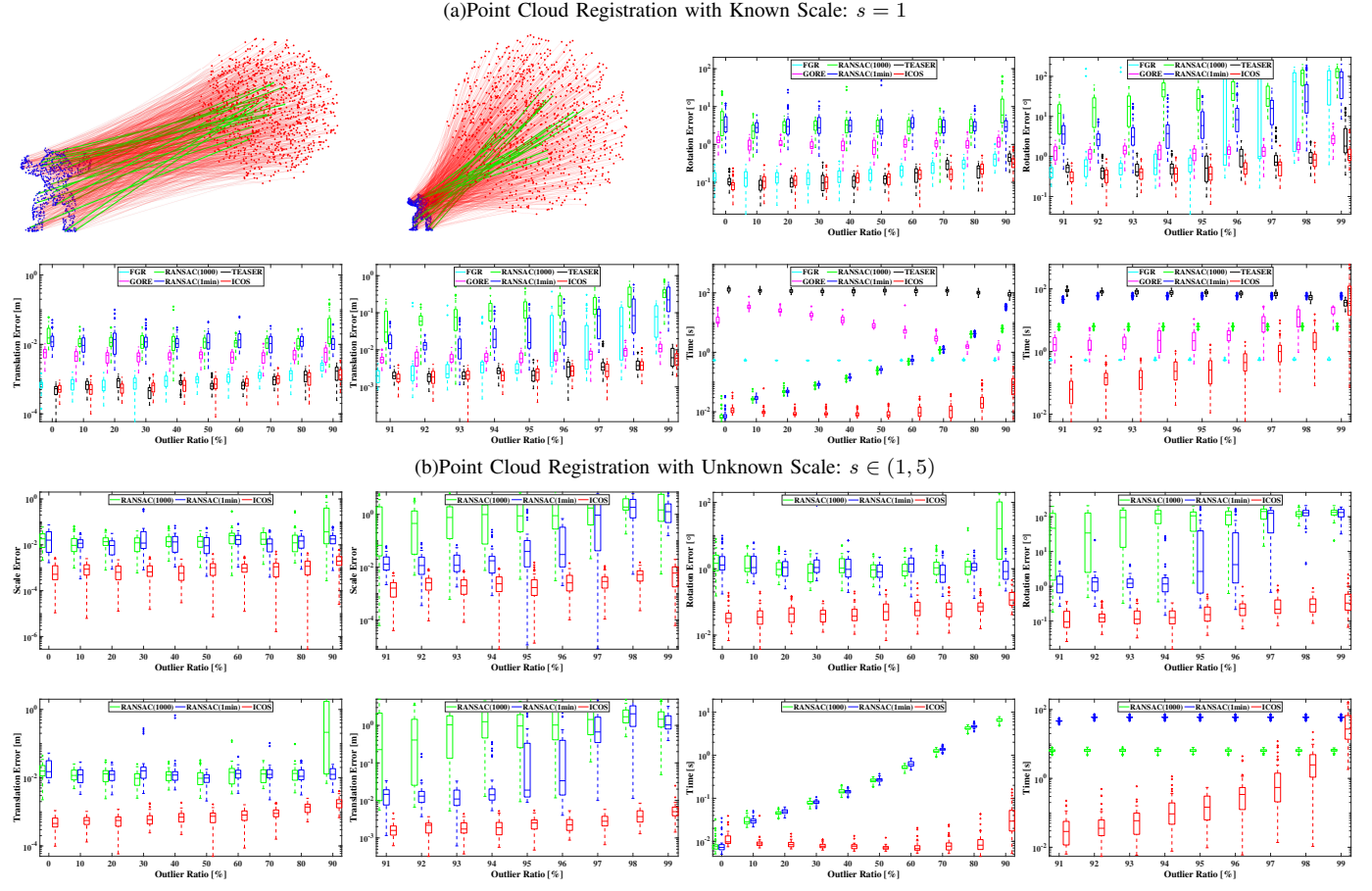


Fig. 6. Benchmarking on the ‘Armadillo’ [13]. Left-top: Examples of a known-scale and an unknown-scale point cloud registration problem with 98% outliers. (a) Known-scale registration results w.r.t. increasing outlier ratio (0-99%). (b) Unknown-scale registration results w.r.t. increasing outlier ratio (0-99%).

from [13], the ‘Mario’ and ‘Duck’ from the SHOT dataset², and the ‘city’ and ‘castle’ from the RGB-D Scans dataset [40].

These experiments are all set up as follows: (i) we first transform a certain point cloud with a random transformation (with both known scale and unknown scale), (ii) we then adopt the FPFH 3D feature descriptor [30] to match and build putative correspondences between the transformed point cloud (colored in magenta) and the initial one (colored in blue), where outliers are bound to exist, and (iii) we apply ICOS to solve the transformation and then reproject the transformed point cloud back to its initial place with the transformation solved. The qualitative results are shown in Fig. 8. Note that after reprojection, the better the magenta point cloud overlaps with the blue one, the smaller the registration errors are.

From Fig. 8, we can see that ICOS provides rather satisfactory robust registration results.

E. Additional Benchmarking on Extreme Noise

We supplement experiments on point cloud registration with extremely high noise. Since the ‘bunny’ point cloud is placed in a $[-0.5, 0.5]^3$ box, adding a noise with $\sigma = 0.1$ is extreme, as demonstrated in Fig. 7, where the shape of the ‘bunny’ is rarely seen. We test ICOS against RANSAC for the unknown-scale registration problems over the high-noise ‘bunny’ with 0-80% outlier ratios, with the results given in Fig. 7.

²<http://vision.deis.unibo.it/list-all-categories/78-cvlab/80-shot>

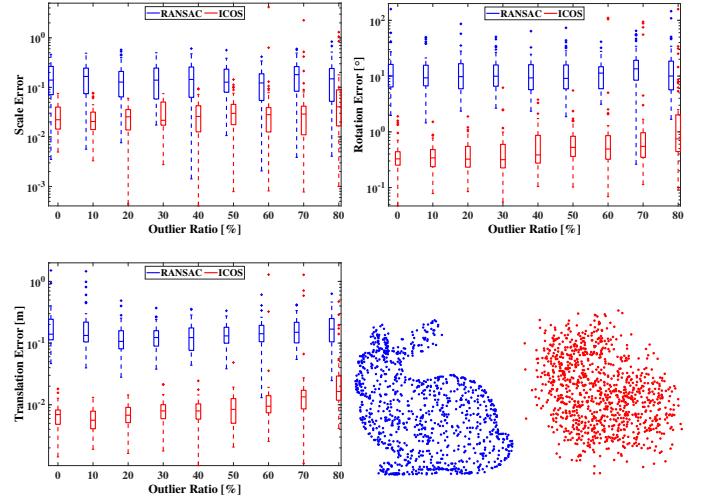


Fig. 7. Results on point cloud registration with extreme noise level. Right-Bottom: The left image is the ‘bunny’ without noise and the right image is that with noise $\sigma = 0.1$.

We can observe that ICOS is still robust against at least 50% outliers with such high noise and succeeds in most cases even at 80%, whereas obviously RANSAC fails even since 0%.

F. Application: 3D Object Localization

We further test ICOS over the RGB-D scenes datasets [22] for dealing with the 3D object localization (pose estimation)

problems. We first extract the 3D point cloud of the targeted object (*cereal box*, *cap*, and *table*) from the scene according to the labels provided and impose a random rigid transformation (with both known scale and unknown scale) as well as random noise with $\sigma = 0.01$ and $\mu = 0$ on the target object. Then, we adopt the FPFH 3D feature descriptor [30] to build putative correspondences between the scene and the transformed object. We find that the correspondences constructed by FPFH contain over 80% outliers in all the scenes tested, and what is worse, the outlier ratios even exceed 90% in some scenes.

For each object-scene registration problem, we apply ICOS, RANSAC(1000) and RANSAC(1min) to estimate the transformation (pose) of the object w.r.t. the scene, and then reproject the object back to the scene with the transformation estimated by each solver, respectively. The qualitative results are demonstrated in Fig. 9 and 10, and the quantitative results are specified in Table. II and III, in which the unit for E_R is degree ($^\circ$), and the unit for E_t is meter, computed as in (22). In each table, the best results are labeled in the **bold** font.

According to the results, ICOS is capable of estimating the object poses robustly and accurately even with as many as over 94% outliers among fewer than 600 correspondences (e.g. *Scene-02*, $s \in (1, 5)$); however, the two RANSAC solvers may fail in some of the cases. Hence, in addition to its superior performance on point cloud registration problems in standard benchmarking, ICOS demonstrates strong practicality for real-world problems.

VII. CONCLUSION

In this paper, we present a novel robust solution ICOS to both the known-scale and unknown-scale point cloud registration problems. We define special compatible structures in the registration problem for creating invariants with mathematical constraints. Then, we are able to render two well-designed invariant-constrained random sampling and inlier seeking frameworks for both the known-scale and unknown-scale problems, which can eliminate outliers by means of fast Boolean conditions and search for qualified 3-COS as well as their 4-COS as the inliers, as our solver ICOS. Generally, ICOS can automatically stop sampling, requiring no change on parameters for different outlier ratios, and eventually return nearly 100% of the inliers out of the entire correspondence set.

We benchmark ICOS against other state-of-the-art point cloud registration solvers in various experiments with multiple point clouds and scenes from real datasets. We show that (i) ICOS can be the most state-of-the-art, or at least one of the most stat-of-the-art, solver for the known-scale registration, since it is robust against 99%, has the best estimation accuracy (at least as accurate as TEASER) and runs fast with 0-98% outliers, and (ii) ICOS demonstrates the similar robustness (99%) and accuracy for the unknown-scale registration, which makes other solvers (e.g. GORE, TEASER) fail at lower than 90% outliers. Also, ICOS has proved to be useful for 3D object localization problems in the RGB-D scenes.

As a matter of fact, ICOS is a promising framework, which applies strategies (e.g. decoupled and constrained random sampling, compatible structures with invariants, stop condition of

sampling in Algorithm 3) that is likely to be extended to other perception problems. Future works may include expanding or improving ICOS as a general-purpose solver for handling multiple geometric problems.

TABLE II
QUANTITATIVE OBJECT LOCALIZATION RESULTS ON THE CEREAL BOX

Scene No.	ICOS	RANSAC(1000)	RANSAC(1min)
<i>Scene-02</i> , $s = 1$ $N = 503$, 93.04%	$E_R = \mathbf{2.420}$ $E_t = \mathbf{0.045}$ $t = \mathbf{0.835}$	$E_R = 22.143$ $E_t = 0.284$ $t = 1.302$	$E_R = 9.475$ $E_t = 0.160$ $t = 19.879$
<i>Scene-05</i> , $s = 1$ $N = 567$, 83.60%	$E_R = \mathbf{1.419}$ $E_t = \mathbf{0.037}$ $t = \mathbf{0.107}$	$E_R = 4.706$ $E_t = 0.106$ $t = 1.451$	$E_R = 5.211$ $E_t = 0.112$ $t = 1.749$
<i>Scene-07</i> , $s = 1$ $N = 284$, 83.45%	$E_R = \mathbf{1.661}$ $E_t = \mathbf{0.040}$ $t = \mathbf{0.248}$	$E_R = 19.245$ $E_t = 0.128$ $t = 1.451$	$E_R = 10.568$ $E_t = 0.293$ $t = 0.756$
<i>Scene-09</i> , $s = 1$ $N = 284$, 90.16%	$E_R = \mathbf{0.899}$ $E_t = \mathbf{0.014}$ $t = 6.562$	$E_R = 18.254$ $E_t = 0.327$ $t = \mathbf{0.968}$	$E_R = 7.029$ $E_t = 0.132$ $t = 5.239$
<i>Scene-02</i> , $s \in (1, 5)$ $N = 584$, 94.86%	$E_R = \mathbf{0.788}$ $E_t = \mathbf{0.022}$ $E_s = \mathbf{0.002}$ $t = \mathbf{0.061}$	$E_R = 95.895$ $E_t = 3.516$ $E_s = 3.261$ $t = 1.496$	$E_R = 177.488$ $E_t = 3.568$ $E_s = 3.289$ $t = 57.422$
<i>Scene-05</i> , $s \in (1, 5)$ $N = 304$, 86.84%	$E_R = \mathbf{0.241}$ $E_t = \mathbf{0.036}$ $E_s = \mathbf{0.016}$ $t = \mathbf{0.051}$	$E_R = 117.781$ $E_t = 5.962$ $E_s = 4.339$ $t = 1.277$	$E_R = 111.556$ $E_t = 5.951$ $E_s = 4.348$ $t = 60.000$
<i>Scene-07</i> , $s \in (1, 5)$ $N = 244$, 83.48%	$E_R = \mathbf{0.511}$ $E_t = \mathbf{0.053}$ $E_s = \mathbf{0.018}$ $t = \mathbf{0.046}$	$E_R = 94.294$ $E_t = 6.851$ $E_s = 3.517$ $t = 0.621$	$E_R = 146.404$ $E_t = 6.919$ $E_s = 3.553$ $t = 0.742$
<i>Scene-09</i> , $s \in (1, 5)$ $N = 674$, 85.46%	$E_R = \mathbf{0.587}$ $E_t = \mathbf{0.053}$ $E_s = \mathbf{0.005}$ $t = \mathbf{0.067}$	$E_R = 2.463$ $E_t = 0.176$ $E_s = 0.074$ $t = 1.759$	$E_R = 1.393$ $E_t = 0.107$ $E_s = 0.063$ $t = 2.953$

TABLE III
QUANTITATIVE OBJECT LOCALIZATION RESULTS ON THE CAP AND THE TABLE

Scene No.	ICOS	RANSAC(1000)	RANSAC(1min)
<i>Scene-01</i> , $s = 1$ $N = 414$, 86.23%	$E_R = \mathbf{0.391}$ $E_t = \mathbf{0.040}$ $t = \mathbf{0.469}$	$E_R = 41.262$ $E_t = 0.637$ $t = 1.074$	$E_R = 4.027$ $E_t = 0.094$ $t = 2.206$
<i>Scene-03</i> , $s = 1$ $N = 366$, 84.15%	$E_R = \mathbf{1.851}$ $E_t = 0.052$ $t = \mathbf{0.796}$	$E_R = 3.876$ $E_t = \mathbf{0.025}$ $t = 0.972$	$E_R = 12.292$ $E_t = 0.249$ $t = 1.276$
<i>Scene-09</i> , $s = 1$ $N = 707$, 85.43%	$E_R = \mathbf{1.626}$ $E_t = \mathbf{0.022}$ $t = \mathbf{0.898}$	$E_R = 24.372$ $E_t = 0.281$ $t = 1.799$	$E_R = 15.531$ $E_t = 0.275$ $t = 3.106$
<i>Scene-12</i> , $s = 1$ $N = 696$, 87.07%	$E_R = \mathbf{0.155}$ $E_t = \mathbf{0.009}$ $t = \mathbf{0.058}$	$E_R = 2.376$ $E_t = 0.027$ $t = 1.776$	$E_R = 8.137$ $E_t = 0.210$ $t = 4.286$
<i>Scene-01</i> , $s \in (1, 5)$ $N = 397$, 93.20%	$E_R = \mathbf{0.680}$ $E_t = \mathbf{0.080}$ $E_s = \mathbf{0.038}$ $t = 2.901$	$E_R = 173.78$ $E_t = 5.237$ $E_s = 3.081$ $t = \mathbf{1.047}$	$E_R = 174.211$ $E_t = 5.284$ $E_s = 3.082$ $t = 17.128$
<i>Scene-03</i> , $s \in (1, 5)$ $N = 316$, 93.35%	$E_R = \mathbf{0.177}$ $E_t = \mathbf{0.026}$ $E_s = \mathbf{0.013}$ $t = \mathbf{0.136}$	$E_R = 168.767$ $E_t = 6.009$ $E_s = 4.950$ $t = 0.863$	$E_R = 169.816$ $E_t = 6.002$ $E_s = 4.955$ $t = 14.769$
<i>Scene-09</i> , $s \in (1, 5)$ $N = 651$, 87.46%	$E_R = \mathbf{0.679}$ $E_t = \mathbf{0.015}$ $E_s = \mathbf{0.067}$ $t = \mathbf{1.823}$	$E_R = 92.402$ $E_t = 1.949$ $E_s = 1.292$ $t = 1.856$	$E_R = 164.111$ $E_t = 1.973$ $E_s = 1.305$ $t = 4.872$
<i>Scene-12</i> , $s \in (1, 5)$ $N = 665$, 85.86%	$E_R = \mathbf{0.053}$ $E_t = \mathbf{0.011}$ $E_s = \mathbf{0.007}$ $t = \mathbf{0.059}$	$E_R = 1.546$ $E_t = 0.089$ $E_s = 0.049$ $t = 1.749$	$E_R = 129.472$ $E_t = 5.515$ $E_s = 3.395$ $t = 3.325$

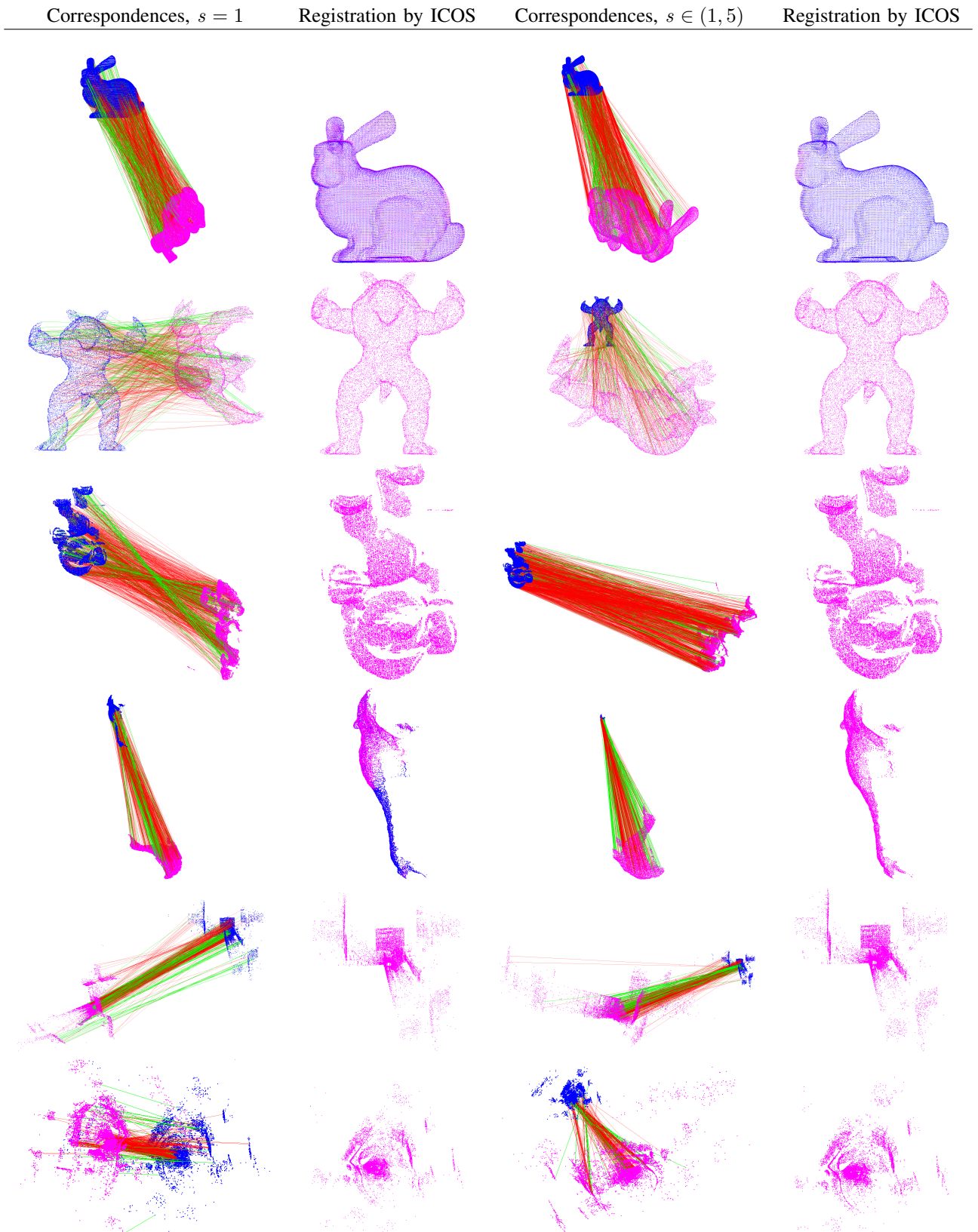


Fig. 8. Qualitative registration results over multiple real datasets. From row 1-6, the point clouds adopted are ‘bunny’, ‘Armadillo’, ‘Mario’, ‘Duck’, ‘city’, and ‘castle’, respectively. Left-Half: Known-scale registration. Right-Half: Unknown-scale registration. In each half, from column 1-2, we display the correspondences (inliers are in green lines and outliers are in red lines), registration (reprojection) result using ICOS, respectively.

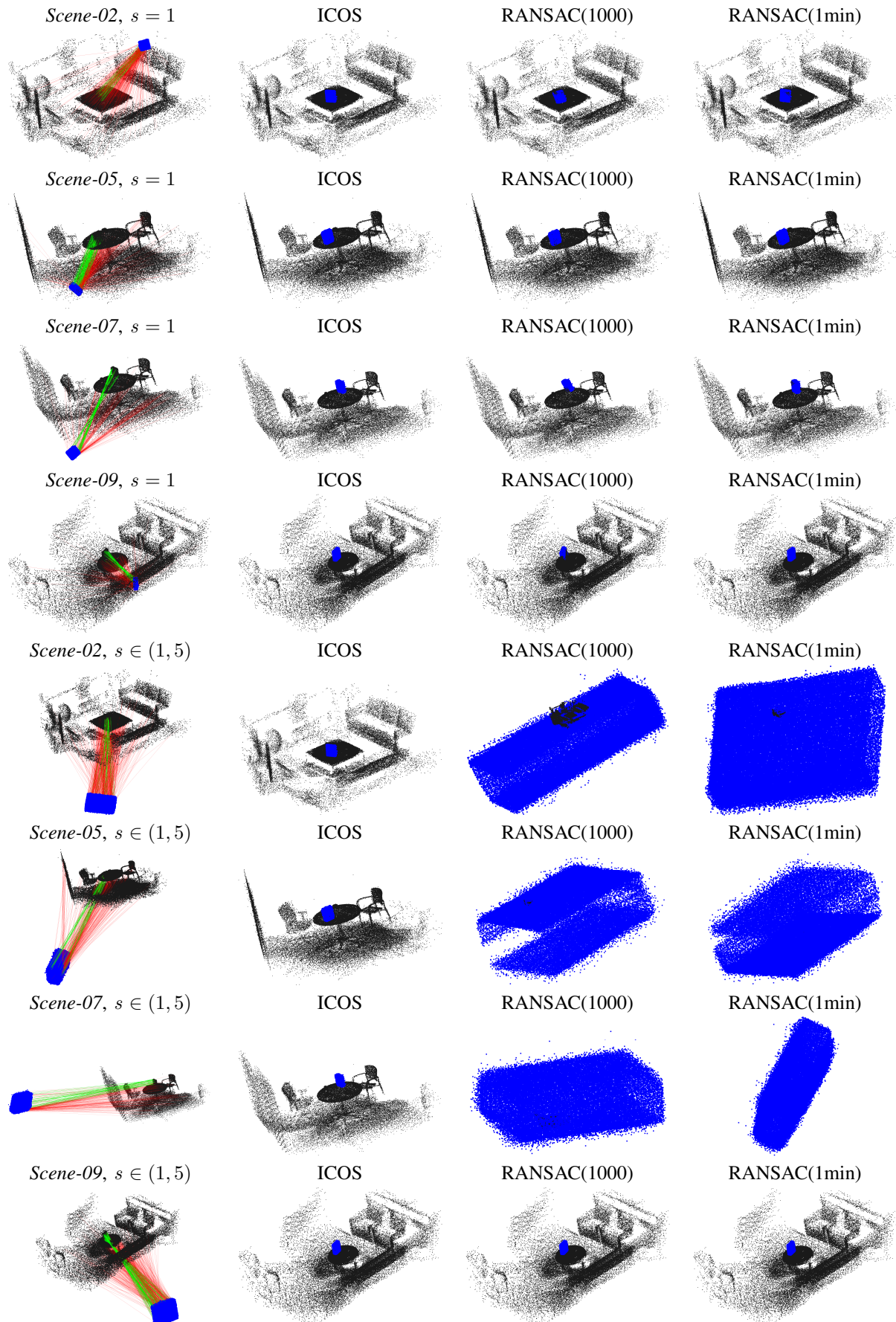


Fig. 9. Qualitative results of 3D object localization (*cereal box*) using ICOS, RANSAC(1000) and RANSAC(1min). From left to right, we show the correspondences (inliers are in green lines and outliers are in red lines), and the registration (reprojection) results with ICOS, RANSAC(1000), and RANSAC(1min), respectively. Note that in all scenes the outlier ratios are over 80%, and our ICOS can always yield promising registration results.

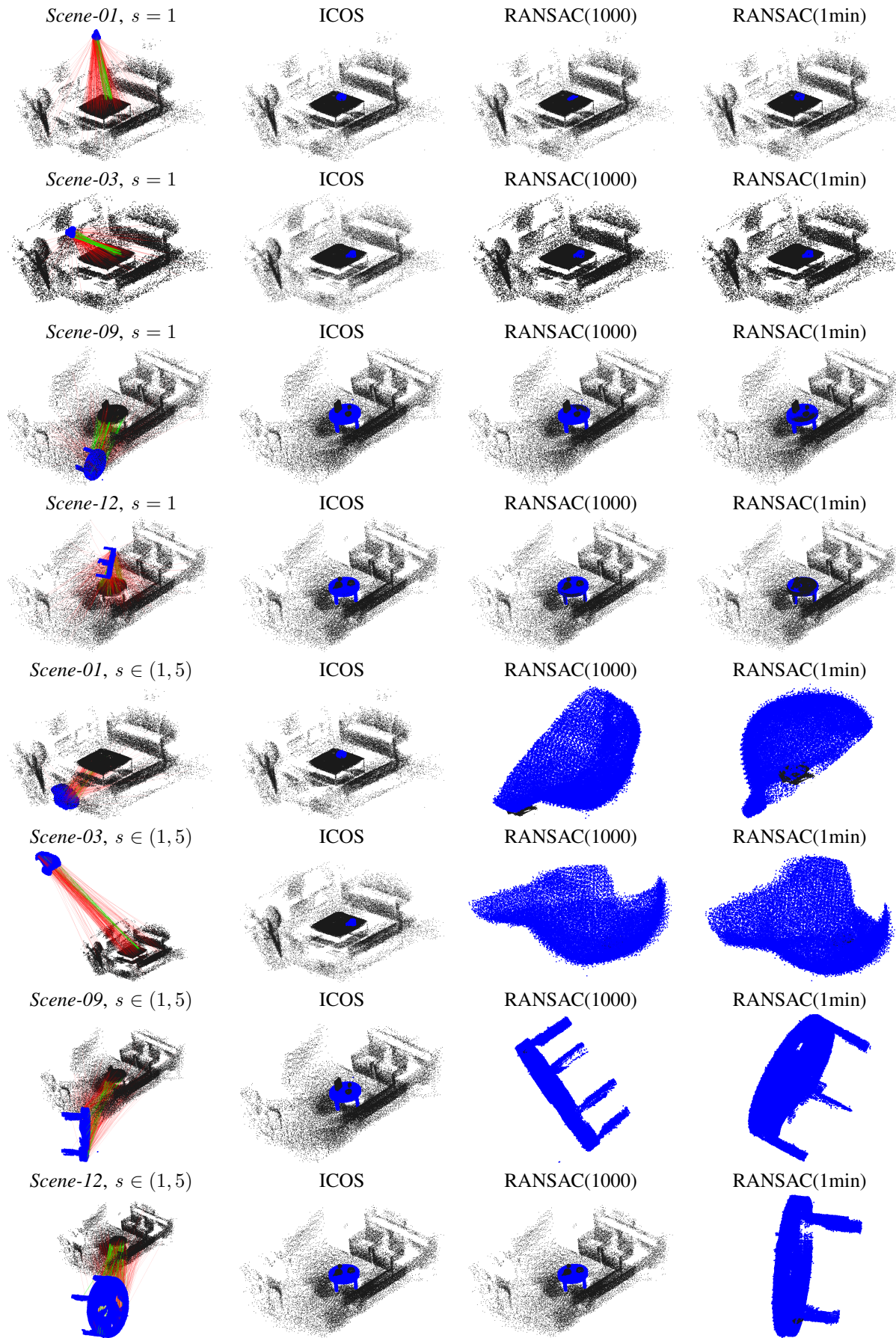


Fig. 10. Qualitative results of 3D object localization (*cap, table*) using ICOS, RANSAC(1000) and RANSAC(1min). From left to right, we show the correspondences (inliers are in green lines and outliers are in red lines), and the registration (reprojection) results with ICOS, RANSAC(1000), and RANSAC(1min), respectively. Note that in all scenes the outlier ratios are over 80%, and our ICOS can always yield promising registration results.

REFERENCES

- [1] Alex M Andrew. Multiple view geometry in computer vision. *Kybernetes*, 2001.
- [2] K Somani Arun, Thomas S Huang, and Steven D Blostein. Least-squares fitting of two 3-d point sets. *IEEE Transactions on pattern analysis and machine intelligence*, (5):698–700, 1987.
- [3] Michel A Audette, Frank P Ferrie, and Terry M Peters. An algorithmic overview of surface registration techniques for medical imaging. *Medical image analysis*, 4(3):201–217, 2000.
- [4] Timothy D Barfoot. *State estimation for robotics*. Cambridge University Press, 2017.
- [5] Herbert Bay, Andreas Ess, Tinne Tuytelaars, and Luc Van Gool. Speeded-up robust features (surf). *Computer vision and image understanding*, 110(3):346–359, 2008.
- [6] PJ Besl and Neil D McKay. A method for registration of 3-d shapes. *IEEE Transactions on Pattern Analysis and Machine Intelligence*, 14(2):239–256, 1992.
- [7] Gérard Blais and Martin D. Levine. Registering multiview range data to create 3d computer objects. *IEEE Transactions on Pattern Analysis and Machine Intelligence*, 17(8):820–824, 1995.
- [8] Jesus Briales and Javier Gonzalez-Jimenez. Convex global 3d registration with lagrangian duality. In *Proceedings of the IEEE Conference on Computer Vision and Pattern Recognition*, pages 4960–4969, 2017.
- [9] Alvaro Parra Bustos and Tat-Jun Chin. Guaranteed outlier removal for point cloud registration with correspondences. *IEEE transactions on pattern analysis and machine intelligence*, 40(12):2868–2882, 2017.
- [10] Sungjoon Choi, Qian-Yi Zhou, and Vladlen Koltun. Robust reconstruction of indoor scenes. In *Proceedings of the IEEE Conference on Computer Vision and Pattern Recognition*, pages 5556–5565, 2015.
- [11] Christopher Choy, Jaesik Park, and Vladlen Koltun. Fully convolutional geometric features. In *Proceedings of the IEEE/CVF International Conference on Computer Vision*, pages 8958–8966, 2019.
- [12] Ondřej Chum, Jiří Matas, and Josef Kittler. Locally optimized ransac. In *Joint Pattern Recognition Symposium*, pages 236–243. Springer, 2003.
- [13] Brian Curless and Marc Levoy. A volumetric method for building complex models from range images. In *Proceedings of the 23rd annual conference on Computer graphics and interactive techniques*, pages 303–312, 1996.
- [14] Bertram Drost, Markus Ulrich, Nassir Navab, and Slobodan Ilic. Model globally, match locally: Efficient and robust 3d object recognition. In *2010 IEEE computer society conference on computer vision and pattern recognition*, pages 998–1005. Ieee, 2010.
- [15] David Eppstein, Maarten Löffler, and Darren Strash. Listing all maximal cliques in sparse graphs in near-optimal time. In *International Symposium on Algorithms and Computation*, pages 403–414. Springer, 2010.
- [16] Martin A Fischler and Robert C Bolles. Random sample consensus: a paradigm for model fitting with applications to image analysis and automated cartography. *Communications of the ACM*, 24(6):381–395, 1981.
- [17] Yulan Guo, Mohammed Bennamoun, Ferdous Sohel, Min Lu, and Jianwei Wan. 3d object recognition in cluttered scenes with local surface features: A survey. *IEEE Transactions on Pattern Analysis and Machine Intelligence*, 36(11):2270–2287, 2014.
- [18] Richard Hartley, Jochen Trumpf, Yuchao Dai, and Hongdong Li. Rotation averaging. *International journal of computer vision*, 103(3):267–305, 2013.
- [19] Peter Henry, Michael Krainin, Evan Herbst, Xiaofeng Ren, and Dieter Fox. Rgb-d mapping: Using kinect-style depth cameras for dense 3d modeling of indoor environments. *The International Journal of Robotics Research*, 31(5):647–663, 2012.
- [20] Berthold KP Horn. Closed-form solution of absolute orientation using unit quaternions. *Josa a*, 4(4):629–642, 1987.
- [21] Peter J Huber. *Robust statistics*, volume 523. John Wiley & Sons, 2004.
- [22] Kevin Lai, Liefeng Bo, Xiaofeng Ren, and Dieter Fox. A large-scale hierarchical multi-view rgb-d object dataset. In *2011 IEEE international conference on robotics and automation*, pages 1817–1824. IEEE, 2011.
- [23] Karel Lebeda, Jiri Matas, and Ondrej Chum. Fixing the locally optimized ransac—full experimental evaluation. In *British machine vision conference*, volume 2. Citeseer, 2012.
- [24] Jiayuan Li, Qingwu Hu, and Mingyao Ai. Point cloud registration based on one-point ransac and scale-annealing biweight estimation. *IEEE Transactions on Geoscience and Remote Sensing*, 2021.
- [25] David G Lowe. Object recognition from local scale-invariant features. In *Proceedings of the seventh IEEE international conference on computer vision*, volume 2, pages 1150–1157. Ieee, 1999.
- [26] Peter Meer. Robust techniques for computer vision. *Emerging topics in computer vision*, pages 107–190, 2004.
- [27] Sushil Mittal, Saket Anand, and Peter Meer. Generalized projection-based m-estimator. *IEEE transactions on Pattern analysis and machine intelligence*, 34(12):2351–2364, 2012.
- [28] Carl Olsson, Fredrik Kahl, and Magnus Oskarsson. Branch-and-bound methods for euclidean registration problems. *IEEE Transactions on Pattern Analysis and Machine Intelligence*, 31(5):783–794, 2008.
- [29] Chavdar Papazov, Sami Haddadin, Sven Parusel, Kai Krieger, and Darius Burschka. Rigid 3d geometry matching for grasping of known objects in cluttered scenes. *The International Journal of Robotics Research*, 31(4):538–553, 2012.
- [30] Radu Bogdan Rusu, Nico Blodow, and Michael Beetz. Fast point feature histograms (fpfh) for 3d registration. In *2009 IEEE international conference on robotics and automation*, pages 3212–3217. IEEE, 2009.
- [31] Radu Bogdan Rusu, Nico Blodow, Zoltan Csaba Marton, and Michael Beetz. Aligning point cloud views using persistent feature histograms. In *2008 IEEE/RSJ international conference on intelligent robots and systems*, pages 3384–3391. IEEE, 2008.
- [32] Jingnan Shi, Heng Yang, and Luca Carlone. Robin: a graph-theoretic approach to reject outliers in robust estimation using invariants. *arXiv preprint arXiv:2011.03659*, 2020.
- [33] Lei Sun. Ransic: Fast and highly robust estimation for rotation search and point cloud registration using invariant compatibility. *arXiv preprint arXiv:2104.09133*, 2021.
- [34] Gary KL Tam, Zhi-Quan Cheng, Yu-Kun Lai, Frank C Langbein, Yonghuai Liu, David Marshall, Ralph R Martin, Xian-Fang Sun, and Paul L Rosin. Registration of 3d point clouds and meshes: a survey from rigid to nonrigid. *IEEE transactions on visualization and computer graphics*, 19(7):1199–1217, 2012.
- [35] Federico Tombari, Samuel Salvi, and Luigi Di Stefano. Performance evaluation of 3d keypoint detectors. *International Journal of Computer Vision*, 102(1-3):198–220, 2013.
- [36] Roberto Tron, David M Rosen, and Luca Carlone. On the inclusion of determinant constraints in lagrangian duality for 3d slam. In *Robotics: Science and Systems (RSS), Workshop The problem of mobile sensors: Setting future goals and indicators of progress for SLAM*, volume 4, 2015.
- [37] Heng Yang, Pasquale Antonante, Vasileios Tzoumas, and Luca Carlone. Graduated non-convexity for robust spatial perception: From non-minimal solvers to global outlier rejection. *IEEE Robotics and Automation Letters*, 5(2):1127–1134, 2020.
- [38] Heng Yang and Luca Carlone. A polynomial-time solution for robust registration with extreme outlier rates. In *Robotics: Science and Systems*, 2019.
- [39] Heng Yang, Jingnan Shi, and Luca Carlone. Teaser: Fast and certifiable point cloud registration. *IEEE Transactions on Robotics*, 2020.
- [40] Bernhard Zeisl, Kevin Koser, and Marc Pollefeys. Automatic registration of rgbd scans via salient directions. In *Proceedings of the IEEE international conference on computer vision*, pages 2808–2815, 2013.
- [41] Ji Zhang and Sanjiv Singh. Loam: Lidar odometry and mapping in real-time. In *Robotics: Science and Systems*, volume 2, 2014.
- [42] Yu Zhong. Intrinsic shape signatures: A shape descriptor for 3d object recognition. In *2009 IEEE 12th International Conference on Computer Vision Workshops, ICCV Workshops*, pages 689–696. IEEE, 2009.
- [43] Qian-Yi Zhou, Jaesik Park, and Vladlen Koltun. Fast global registration. In *European Conference on Computer Vision*, pages 766–782. Springer, 2016.